

# Better Batch for Deep Probabilistic Time Series Forecasting

Vincent Zhihao Zheng  
CIRRELT and McGill University

Seongjin Choi  
University of Minnesota

Lijun Sun  
CIRRELT and McGill University

## Abstract

Deep probabilistic time series forecasting has gained significant attention due to its superior performance in nonlinear approximation and its ability to provide valuable uncertainty quantification for decision-making tasks. However, many existing models oversimplify the problem by assuming that the error process is time-independent, thereby overlooking the serial correlation in the error process. To overcome this limitation, we propose an innovative training method that incorporates error autocorrelation to further enhance the accuracy of probabilistic forecasting. Our method involves constructing a mini-batch as a collection of  $D$  consecutive time series segments for model training and explicitly learning a time-varying covariance matrix over each mini-batch that encodes the error correlation among adjacent time steps. The learned covariance matrix can be used to improve prediction accuracy and enhance uncertainty quantification. We evaluate our method on two different neural forecasting models and multiple public datasets, and the experimental results confirm the effectiveness of the proposed approach in enhancing the performance of both models across a wide range of datasets, yielding notable improvements in predictive accuracy.

## 1 INTRODUCTION

Time series forecasting has gained significant attention in the field of deep learning due to its wide-ranging applications (Benidis et al., 2022). Essentially, time series forecasting tasks can be classified into determini-

istic forecasting and probabilistic forecasting. Deterministic forecasting provides point estimates for future time series values, while probabilistic forecasting goes a step further by providing a distribution that quantifies the uncertainty associated with the predictions. As additional information on uncertainty assists users in making more informed decisions, probabilistic forecasting has become increasingly attractive and extensive efforts have been made to enhance uncertainty quantification. In time series analysis, errors can exhibit correlation for various reasons, such as the omission of essential covariates or model inaccuracy. Autocorrelation (also known as serial correlation) and contemporaneous correlation are two common types of correlation in multivariate time series forecasting. Autocorrelation captures the temporal correlation present in errors, whereas contemporaneous correlation refers to the correlation among different time series at the same time.

This paper primarily investigates the issue of autocorrelation in errors. Modeling error autocorrelation is an important research question in statistical time series models. One common approach to address this issue is assuming that the error series of the base model follows an autoregressive integrated moving average (ARIMA) process, with the remaining errors assumed to be independent (Hyndman and Athanasopoulos, 2018). Similar challenges may arise in learning nonlinear deep learning (DL)-based forecasting models. To address this issue, previous studies have attempted to incorporate autocorrelation in deterministic time series forecasting by modifying the loss function through dynamic regression (Sun et al., 2021; Zheng et al., 2023). However, since both the neural network and the correlated errors can explain the data, these models may face challenges in balancing the two sources in the absence of an overall covariance structure. Moreover, these methods are not readily applicable to probabilistic forecasting models, where the model output typically consists of parameters of the predictive distribution rather than the actual time series values.

In this paper, we propose a novel batch structure that allows us to explicitly model error autocorrelation.

Each batch comprises multiple mini-batches, with each mini-batch grouping a fixed number of consecutive training instances. Our main idea draws inspiration from the generalized least squares (GLS) method used in linear regression models with dependent errors. We extend the Gaussian likelihood of a univariate model to a multivariate Gaussian likelihood by incorporating a time-varying covariance matrix that encodes error autocorrelation within a mini-batch. The covariance matrix is decomposed into two components, a scale vector and a correlation matrix, that are both time-varying. In particular, we parameterize the correlation matrix using a weighted sum of several base kernel matrices, and the weights are dynamically generated from the output of the base probabilistic forecasting model. This enables us to improve the accuracy of estimated distribution parameters during prediction by using the learned dynamic covariance matrix to account for previously observed residuals. By explicitly modeling dynamic error covariance, our method enhances training flexibility, improves time series prediction accuracy, and provides high-quality uncertainty quantification. Our main contributions are as follows:

- We propose a novel method that enhances the training and prediction of univariate probabilistic time series models by learning a time-varying covariance matrix that captures the correlated errors within a mini-batch.
- We parameterize the dynamic correlation matrix with a weighted sum of several base kernel matrices. This ensures that the correlation matrix is a positive definite symmetric matrix with unit diagonals. This approach allows us to jointly learn the dynamic weights alongside the base model.
- We evaluate the effectiveness of the proposed approach on two base models with distinct architectures, DeepAR and Transformer, on multiple public datasets. Our method effectively captures the autocorrelation in errors and thus offers enhanced prediction quality. Importantly, these improvements are realized through a statistical formulation without substantially increasing the number of parameters in the model.

## 2 PRELIMINARIES

### 2.1 Probabilistic Time Series Forecasting

Denote  $\mathbf{z}_t = [z_{1,t}, \dots, z_{N,t}]^\top \in \mathbb{R}^N$  the vector containing the values of a multivariate time series at time step  $t$ , where  $N$  is the number of time series. Given the observed history  $\{\mathbf{z}_t\}_{t=1}^T$ ,

probabilistic time series forecasting can be formulated as estimating the joint conditional distribution  $p(\mathbf{z}_{T+1:T+Q} \mid \mathbf{z}_{T-P+1:T}; \mathbf{x}_{T-P+1:T+Q})$ , where  $\mathbf{z}_{t_1:t_2} = [\mathbf{z}_{t_1}, \dots, \mathbf{z}_{t_2}]$  and  $\mathbf{x}_t$  are some known time-dependent covariates (e.g., time of day and day of week). In other words, we are interested in forecasting  $Q$  future values given  $P$  historical values and covariates. The model can be further factorized as

$$\begin{aligned} p(\mathbf{z}_{T+1:T+Q} \mid \mathbf{z}_{T-P+1:T}; \mathbf{x}_{T-P+1:T+Q}) \\ = \prod_{t=T+1}^{T+Q} p(\mathbf{z}_t \mid \mathbf{z}_{t-P:t-1}; \mathbf{x}_{t-P:t}), \end{aligned} \quad (1)$$

which is an autoregressive model that can be used for either one-step-ahead ( $Q = 1$ ) or multi-step-ahead forecasting in a rolling manner. When used in multi-step-ahead prediction, samples are drawn for the prediction range ( $t \geq T + 1$ ) and fed back for the next time step until the end of the prediction range. The conditioning is usually encapsulated into a state vector  $\mathbf{h}_t$  of a transition dynamics  $f_\Theta$  that evolves over time  $\mathbf{h}_t = f_\Theta(\mathbf{h}_{t-1}, \mathbf{z}_{t-1}, \mathbf{x}_t)$ . Therefore, Eq. (1) can be simplified as

$$\begin{aligned} p(\mathbf{z}_{T+1:T+Q} \mid \mathbf{z}_{T-P+1:T}; \mathbf{x}_{T-P+1:T+Q}) \\ = \prod_{t=T+1}^{T+Q} p(\mathbf{z}_t \mid \mathbf{h}_t), \end{aligned} \quad (2)$$

where  $\mathbf{h}_t$  is mapped to the parameters of a chosen parametric distribution (e.g., Gaussian, Poisson). When  $N = 1$ , the problem is reduced to a univariate model

$$\begin{aligned} p(\mathbf{z}_{i,T+1:T+Q} \mid \mathbf{z}_{i,T-P+1:T}; \mathbf{x}_{i,T-P+1:T+Q}) \\ = \prod_{t=T+1}^{T+Q} p(z_{i,t} \mid \mathbf{h}_{i,t}), \end{aligned} \quad (3)$$

where  $i$  is the identifier of a time series.

### 2.2 Error Autocorrelation

In the majority of probabilistic time series forecasting literature, the data under consideration is typically continuous, and the errors are assumed to follow an independent Gaussian distribution. Consequently, the time series variable associated with this framework is expected to follow a Gaussian distribution as well:

$$z_{i,t} \mid \mathbf{h}_{i,t} \sim \mathcal{N}(\mu(\mathbf{h}_{i,t}), \sigma^2(\mathbf{h}_{i,t})), \quad (4)$$

where  $\mu(\cdot)$  and  $\sigma(\cdot)$  map the state vector  $\mathbf{h}_{i,t}$  to the mean and standard deviation of a Gaussian distribution. For instance, the DeepAR model (Salinas et al., 2020) adopts  $\mu(\mathbf{h}_{i,t}) = \mathbf{w}_\mu^\top \mu(\mathbf{h}_{i,t}) + b_\mu$  and

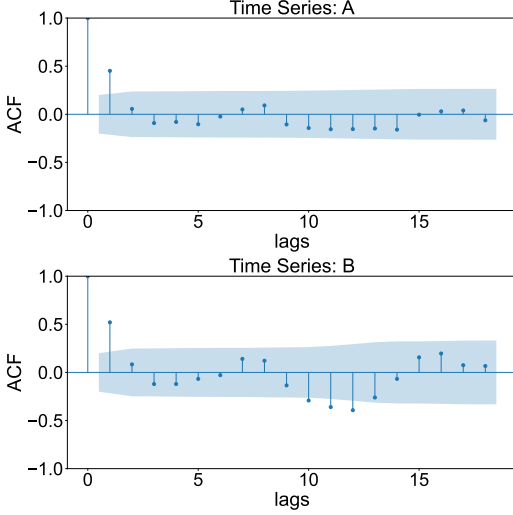


Figure 1: Autocorrelation function (ACF) of the one-step-ahead prediction residuals from two time series in the `m4_hourly` dataset, computed using prediction results of DeepAR. The shaded area highlights the 95% confidence interval, denoting regions where the correlation is statistically insignificant.

$\sigma(\mathbf{h}_{i,t}) = \log(1 + \exp(\mathbf{w}_\sigma^\top \mathbf{h}_{i,t} + b_\sigma))$  and both parameters are time-varying. This formulation is equivalent to decompose  $z_{i,t} = \mu_{i,t} + \eta_{i,t}$  with  $\eta_{i,t} \sim \mathcal{N}(0, \sigma_{i,t}^2)$ . Assuming the errors to be independent corresponds to  $\text{Cov}(\eta_{i,t-\Delta}, \eta_{i,t}) = 0, \forall \Delta \neq 0$ . In the following of this paper, we focus on this setting with Gaussian errors.

When there exists serial correlation in the error process, we will have  $\boldsymbol{\eta}_{T+1:T+Q} = [\eta_{i,T+1}, \dots, \eta_{i,T+Q}]^\top$  follows a multivariate Gaussian distribution  $\mathcal{N}(\mathbf{0}, \boldsymbol{\Sigma})$ , where  $\boldsymbol{\Sigma}$  is the covariance matrix. Fig. 1 gives an example of residual autocorrelation functions (ACF) calculated using the prediction results from DeepAR on the `m4_hourly` dataset for two time series. The plot reveals a prevalent issue of lag-1 autocorrelation. Ignoring the systematic autocorrelation will undermine the performance of forecasting.

### 3 RELATED WORK

#### 3.1 Probabilistic Time Series Forecasting

Probabilistic forecasting aims to provide the probability distribution of the target variable instead of generating a single-point estimate as in deterministic forecasting. Essentially, there are two approaches to achieve this, through the probability density function (PDF) and through the quantile function (Benidis et al., 2022). For instance, MQ-RNN (Wen et al., 2017) directly generates quantile forecasts using a sequence-to-sequence (Seq2Seq) recurrent neu-

ral network (RNN) architecture. The PDF-based approaches, which are widely used, often assume a specific distribution form for the target variables and utilize neural networks to generate the parameters of the distribution. DeepAR (Salinas et al., 2020) is a notable example that employs an RNN architecture to model hidden state transitions. At each time step, the hidden state is used to conditionally generate the parameters of a Gaussian distribution, from which prediction samples are drawn. DeepVAR (Salinas et al., 2019), the multivariate version of DeepAR, utilizes Gaussian copula to construct a joint cumulative distribution by mapping the original variables to marginally uniform variables. In addition to outputting distribution parameters, neural networks can be used to generate probabilistic model parameters. For example, the deep state space model (SSM) (Rangapuram et al., 2018) utilizes RNNs to generate SSM parameters, enabling the generation of prediction samples. Normalizing Kalman Filter (NKF) (de Bézenac et al., 2020) combines normalizing flows (NFs) with the classical linear Gaussian state space model to model nonlinear dynamics and evaluate the probability density function of observations. The RNNs in the NKF model generate the parameters at each time step. The deep factor model (Wang et al., 2019) consists of a fixed global component and a random component, which can be any classic probabilistic time series model such as a Gaussian noise process. The global component, parameterized by neural networks, combines deterministic factors, while the random component forms the latent function that conditions a parametric distribution to generate observations. Some approaches aim to provide more expressive conditioning for probabilistic forecasting, such as using Transformer to replace RNNs to model the dynamics of latent states, thus breaking the Markovian assumption in RNNs (Tang and Matteson, 2021). Another avenue to improve probabilistic forecasting centers on adopting more intricate distribution forms, including normalizing flows (Rasul et al., 2020) and diffusion models (Rasul et al., 2021). We refer readers to Benidis et al. (2022) for a recent and comprehensive review.

#### 3.2 Modeling Correlated Errors

The issue of error correlation in time series data has been extensively studied in the fields of econometrics and statistics (Prado et al., 2021; Hyndman and Athanasopoulos, 2018; Hamilton, 2020). Autocorrelation, also known as serial correlation, captures the correlation of errors over time in a time series. Contemporaneous correlation refers to the correlation among a set of time series variables in the same time period. Statistical frameworks, such as autoregressive (AR) and moving average (MA) models, along with

their multivariate counterparts, have been well developed in statistics to address these correlation issues. Several recent DL-based time series models have also tried to explicitly model error correlation structures to enhance forecasting performance. For example, in Sun et al. (2021), the input and output of a neural network are re-parameterized to model first-order error autocorrelation in time series, thus capturing serially correlated errors with an AR(1) process. This technique enhances the performance of DL-based one-step-ahead forecasting models, enabling joint optimization of the base and error regressors. The method has been extended to multivariate models for Seq2Seq time series forecasting tasks, assuming a matrix AR process for the error matrix (Zheng et al., 2023). In terms of learning contemporaneous correlation, researchers have proposed modeling error correlation using a multivariate Gaussian distribution in node regression problems (Jia and Benson, 2020). The resulting method, called error propagation in Graph Neural Networks (GNNs), adjusts the prediction of unknown nodes based on known node labels. Similarly, a correct-and-smooth model was proposed for classification tasks, correcting correlated errors in GNNs (Huang et al., 2020). Generalized Least Squares (GLS) loss is introduced in (Zhan and Datta, 2023) to capture spatial correlation of errors in neural networks for geospatial data, which bridges deep learning with Gaussian processes. GLS can also be integrated into other nonlinear regression models, such as random forest Saha et al. (2023). In Choi et al. (2022), a dynamic mixture of matrix normal distributions was proposed to characterize spatiotemporally correlated errors in Seq2Seq models.

To our knowledge, our work presents a novel exploration of addressing error autocorrelation in probabilistic time series forecasting through the development of innovative training schemes. Our proposed method is closely related to the methods presented in Sun et al. (2021), Saha et al. (2023) and Zhan and Datta (2023). Saha et al. (2023) proposed to use GLS in training random forests for spatial and temporal data, assuming the residual covariance is known in advance. Sun et al. (2021) models residual correlation by introducing a fixed AR coefficient and modifying the loss function. Zhan and Datta (2023) extended the GLS training scheme to spatial data and developed a graph neural network model for efficient training. Compared with these prior works, our method focuses on learning a dynamic covariance matrix for a mini-batch with autocorrelated errors, which is learned together with the mean prediction. The introduction of the error covariance matrix not only provides a statistical framework for characterizing error autocorrelation but also enhances prediction accuracy.

## 4 OUR METHOD

Our approach is based on the formulation presented in Eq. (3), using an autoregressive model as the base model. Given the primary focus of this paper on univariate models, we will omit the subscript  $i$  for the remainder of this paper. In a general sense, an autoregressive probabilistic forecasting model comprises two key components: firstly, a transition model (e.g., an RNN) to characterize state transitions  $\mathbf{h}_t$ , and secondly, a distribution head  $\theta$  responsible for mapping  $\mathbf{h}_t$  to the parameters governing the desired distribution. Furthermore, the encoder-decoder framework is employed to facilitate multi-step forecasting, wherein an input sequence spanning  $P$  time steps is used to generate an output sequence spanning  $Q$  time steps. The likelihood is expressed as  $p(z_t | \theta(\mathbf{h}_t))$  for an individual observation, and in the case of employing a Gaussian distribution,  $\theta(\mathbf{h}_t)$  takes the form of  $(\mu_t, \sigma_t)$ . In the training batch, the target time series variable can be modeled as

$$z_t = \mu_t + \sigma_t \epsilon_t. \quad (5)$$

Gaussian likelihood-based models are built on the assumption that  $\epsilon_t = \frac{z_t - \mu_t}{\sigma_t} \stackrel{\text{iid}}{\sim} \mathcal{N}(0, 1)$ , which implies that  $\epsilon_t$  are independent and identically distributed according to a standard normal distribution. Model training can be achieved by maximizing the log-likelihood

$$\mathcal{L} = \sum_{t=1}^T \log p(z_t | \theta(\mathbf{h}_t)) \propto \sum_{t=1}^T -\frac{1}{2} \epsilon_t^2 - \ln \sigma_t. \quad (6)$$

We adopt a unified univariate model trained across all time series, rather than training individual models for each time series. Moreover, if we assume the error process to be isotropic, the loss function is equivalent to the Mean Squared Error (MSE) commonly employed in training deterministic models (Sun et al., 2021). However, this assumption of independence ignores the potential serial correlation in  $\epsilon_t$ .

### 4.1 Training with Mini-batch

We propose a novel training approach by constructing mini-batches instead of using individual training instances. For most existing deep probabilistic time series models including DeepAR, each training instance consists of a time series segment with a length of  $P+Q$ , where  $P$  represents the conditioning range and  $Q$  denotes the prediction range. However, as mentioned, this simple approach cannot characterize the serial correlation of errors among consecutive time steps. To address this issue, we group  $D$  consecutive time series segments into a mini-batch, with each segment having

a length of  $P + 1$  (i.e.,  $Q = 1$ ). In other words, the new training instance (i.e., a mini-batch) becomes a collection of  $D$  time series segments with a prediction range  $Q = 1$ . The composition of a mini-batch is illustrated in Fig. 2. An example of the collection of target variables in a mini-batch of size  $D$  (the time horizon we use for capturing serial correlation) is given by

$$\begin{aligned} z_t &= \mu_t + \sigma_t \epsilon_t, \\ z_{t+1} &= \mu_{t+1} + \sigma_{t+1} \epsilon_{t+1}, \\ &\dots \\ z_{t+D-1} &= \mu_{t+D-1} + \sigma_{t+D-1} \epsilon_{t+D-1}, \end{aligned} \quad (7)$$

where for time point  $t'$ ,  $\mu_{t'}$  and  $\sigma_{t'}$  are the output of the model for each time series segment in the mini-batch, and  $\epsilon_{t'}$  is the normalized error term. We use boldface symbols to denote the vectors of data and parameters in this mini-batch, e.g.,  $\mathbf{z}_t^{\text{bat}} = [z_t, z_{t+1}, \dots, z_{t+D-1}]^\top$  and the same notation applies to  $\boldsymbol{\mu}_t^{\text{bat}}$  and  $\boldsymbol{\sigma}_t^{\text{bat}}$ .

Rather than assuming independence among the normalized errors, we consider modeling the joint distribution of the error vector in a mini-batch  $\boldsymbol{\epsilon}_t$ , denoted as  $\boldsymbol{\epsilon}_t^{\text{bat}} = [\epsilon_t, \epsilon_{t+1}, \dots, \epsilon_{t+D-1}]^\top \sim \mathcal{N}(\mathbf{0}, \mathbf{C}_t)$ , where  $\mathbf{C}_t$  is a time-varying correlation matrix. To efficiently characterize the time-varying patterns, we parameterize  $\mathbf{C}_t$  as a dynamic weighted sum of several base kernel matrices:  $\mathbf{C}_t = \sum_{m=1}^M w_{m,t} \mathbf{K}_m$ , where  $w_{m,t} \geq 0$  (with  $\sum_m w_{m,t} = 1$ ) represents the component weights. For simplicity, we model each base component  $\mathbf{K}_m$  using a kernel matrix generated from a squared-exponential (SE) kernel function,  $\mathbf{K}_m^{ij} = \exp(-\frac{(i-j)^2}{l^2})$ , with different lengthscales  $l$  (e.g.,  $l = 1, 2, 3, \dots$ ). Additionally, we include an identity matrix in the additive structure to capture the independent noise process. Taken together, this parameterization ensures that  $\mathbf{C}_t$  is a positive definite symmetric matrix with unit diagonals, thus being a valid correlation matrix. A small neural network is attached to the original model to project the hidden state to the weights by setting the number of nodes in the final hidden layer to  $M$  (i.e., the number of components). A softmax layer is used as the output layer to ensure that these weights sum up to 1. The parameters of the small neural network can be learned jointly with the base model.

The utilization of a time-varying correlation matrix, as opposed to a static correlation matrix, offers the advantage of enabling the model to adapt dynamically to the evolving structure of the error process. For example, the model can assign a higher weight to a kernel matrix generated by a kernel function with a lengthscale of  $l = 3$  when strong and long-range correlations are present in the current context, whereas it can favor the identity matrix when errors

become white noise. This parameterization empowers the model to capture positive autocorrelation that diminishes over time lags. Alternatively, one could opt for a fully learnable positive definite symmetric Toeplitz matrix to parameterize the correlation matrix, which can also accommodate negative and complex correlations. With this formulation, the distribution of  $\boldsymbol{\epsilon}_t$  becomes a multivariate Gaussian, which also leads to  $\mathbf{z}_t^{\text{bat}} \sim \mathcal{N}(\boldsymbol{\mu}_t^{\text{bat}}, \boldsymbol{\Sigma}_t^{\text{bat}})$ . The  $D \times D$  covariance of the associated target variables can be decomposed as  $\boldsymbol{\Sigma}_t^{\text{bat}} = \text{diag}(\boldsymbol{\sigma}_t^{\text{bat}}) \mathbf{C}_t \text{diag}(\boldsymbol{\sigma}_t^{\text{bat}})$ . As both  $\boldsymbol{\mu}_t^{\text{bat}}$  and  $\boldsymbol{\sigma}_t^{\text{bat}}$  are default outputs of the base probabilistic model, the likelihood for a specific time series can be constructed for each mini-batch, and the overall likelihood is given by:

$$\mathcal{L} = \sum_{t=1}^{T-D+1} \log p(\mathbf{z}_t^{\text{bat}} | \boldsymbol{\mu}_t^{\text{bat}}, \boldsymbol{\Sigma}_t^{\text{bat}}). \quad (8)$$

By allowing overlap, a total of  $T - D + 1$  mini-batches can be generated for each time series from the training data.

## 4.2 Multi-step Rolling Prediction

An autoregressive model performs forecasting in a rolling manner, i.e., a sample of the target variable is drawn at each time step and fed to the next time step as input until reaching the desired prediction range. Our method can provide extra calibration for this process given the learned correlation matrix  $\mathbf{C}_t$ . Assume that we have observations till time step  $t$  and recall that the collection of normalized errors in a mini-batch jointly follows a multivariate Gaussian. Thus, for the first time step ( $t+1$ ) to be predicted, we have the conditional distribution of  $\epsilon_{t+1}$  given the past  $D-1$  errors using the conditional distribution of jointly Gaussian variables:

$$\begin{aligned} \epsilon_{t+1} | \epsilon_t, \epsilon_{t-1}, \dots, \epsilon_{t-D+2} \\ \sim \mathcal{N}(\mathbf{C}_* \mathbf{C}_{\text{obs}}^{-1} \boldsymbol{\epsilon}_{\text{obs}}, 1 - \mathbf{C}_* \mathbf{C}_{\text{obs}}^{-1} \mathbf{C}_*^\top), \end{aligned} \quad (9)$$

where  $\boldsymbol{\epsilon}_{\text{obs}} = [\epsilon_{t-D+2}, \dots, \epsilon_{t-1}, \epsilon_t]^\top \in \mathbb{R}^{D-1}$  is the collection of observed residuals, which will be accessible/available when forecasting step  $t+1$ . Here,  $\mathbf{C}_{\text{obs}}$  corresponds to the  $(D-1) \times (D-1)$  partition of  $\mathbf{C}_{t+1}$  that describes the correlation within  $\boldsymbol{\epsilon}_{\text{obs}}$ , and  $\mathbf{C}_*$  corresponds to the  $(D-1) \times 1$  partition of  $\mathbf{C}_{t+1}$  that describes the correlation between  $\epsilon_{t+1}$  and  $\boldsymbol{\epsilon}_{\text{obs}}$ , i.e.,  $\mathbf{C}_{t+1} = \begin{bmatrix} \mathbf{C}_{\text{obs}} & \mathbf{C}_*^\top \\ \mathbf{C}_* & 1 \end{bmatrix}$ . Note that for brevity we remove the time index  $t$  in  $\mathbf{C}_{\text{obs}}$ ,  $\mathbf{C}_*$  and  $\boldsymbol{\epsilon}_{\text{obs}}$ . The weights for generating  $\mathbf{C}_{t+1}$  are obtained from the hidden state of the base model at time step  $t+1$ . As both  $\mu_{t+1}$  and  $\sigma_{t+1}$  are deterministic output variables from

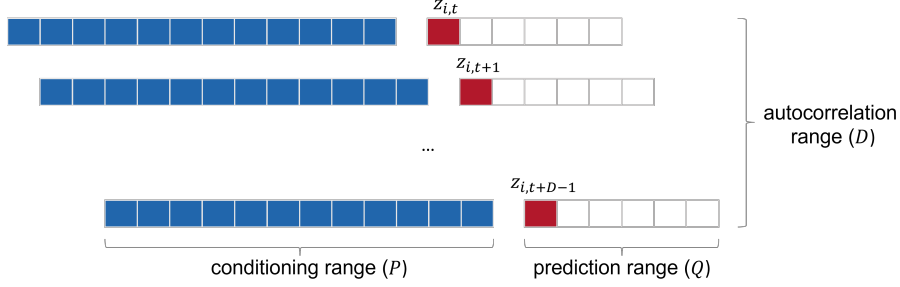


Figure 2: Example of a mini-batch. Colored parts denote the time series segments that construct the mini-batch. Each mini-batch has a time span of  $P + D$ , and only one-step-ahead prediction is involved during training.

the base model, we can first draw a sample  $\tilde{\epsilon}_{t+1}$  from Eq. (9), and then transform it to target variable by

$$\tilde{z}_{t+1} = \mu_{t+1} + \sigma_{t+1} \tilde{\epsilon}_{t+1}. \quad (10)$$

As can be seen, the final distribution for  $z_{t+1}$  becomes

$$z_{t+1} \mid \mathbf{h}_{t+1}, \epsilon_{\text{obs}} \sim \mathcal{N}(\bar{\mu}_{t+1}, \bar{\sigma}_{t+1}^2), \quad (11)$$

where

$$\begin{aligned} \bar{\mu}_{t+1} &= \mu_{t+1} + \sigma_{t+1} \mathbf{C}_* \mathbf{C}_{\text{obs}}^{-1} \epsilon_{\text{obs}}, \\ \bar{\sigma}_{t+1}^2 &= \sigma_{t+1}^2 \left(1 - \mathbf{C}_* \mathbf{C}_{\text{obs}}^{-1} \mathbf{C}_*^\top\right). \end{aligned} \quad (12)$$

Following this approach, multi-step-ahead forecasting can be achieved by treating the sample  $\tilde{\epsilon}_{t+1}$  as an observation and continuing the process to obtain a trajectory of  $\{\tilde{\epsilon}_{t+q}\}_{q=1}^Q$ .

## 5 EXPERIMENTS

### 5.1 Datasets and Models

We integrate the proposed framework into DeepAR (Salinas et al., 2020) and an autoregressive decoder-only Transformer (i.e., the GPT model (Radford et al., 2018)) as base prediction models. A Gaussian distribution head is employed to generate the distribution parameters for probabilistic forecasting based on the hidden state outputted by the model. It should be noted that our approach can be applied to other autoregressive univariate models without any loss of generality, as long as the final prediction follows a Gaussian distribution. We implemented these models using PyTorch Forecasting (Beitner, 2020). Both models utilize input data consisting of lagged time series values from the preceding time step, accompanied by supplementary features including time of day, day of the week, global time index, and unique time series identifiers. We refer readers to the supplementary material for comprehensive information on the experiment setup.

To evaluate the effectiveness of our approach, we conduct a comprehensive set of experiments on a diverse

set of real-world time series data obtained from GluonTS (Alexandrov et al., 2020, please refer to supplementary material for dataset details). These datasets have gained widespread recognition for benchmarking time series forecasting models. The prediction range ( $Q$ ) and the number of rolling evaluations for each dataset were determined based on their respective configurations within GluonTS. For each dataset, we performed a sequential split into training, validation, and testing sets, with the temporal length of the validation set being the same as that of the testing sets. The testing horizon was determined based on the prediction range and the required number of rolling evaluations. For example, the testing horizon for **traffic** is computed as  $24 + 7 - 1 = 30$  time steps. Therefore, the model will be tested for predicting 24 steps ( $Q$ ) in a rolling manner with 7 different consecutive prediction start timestamps. The data is standardized using the mean and standard deviation obtained from each time series within the training set. Subsequently, the predictions were rescaled to their original values for the computation of evaluation metrics.

### 5.2 Evaluation against Baseline

We evaluate the proposed approach by comparing it with models trained using Gaussian likelihood loss. To simplify the comparison and ensure fairness in terms of the data used during training, we set the autocorrelation range ( $D$ ) to be identical to the prediction range ( $Q$ ). This alignment ensures that each mini-batch in our method covers a time horizon of  $P + D$ , while in the conventional training method, each training instance spans a time horizon of  $P + Q$ . By setting  $D = Q$ , we guarantee that both methods involve the same amount of data per batch, given the same batch sizes. Furthermore, we follow the default configuration in GluonTS by setting the context range equal to the prediction range, i.e.,  $P = Q$ .

In our proposed method, we introduce a small number of additional parameters dedicated to projecting

the hidden state into component weights  $w_{m,t}$ , which play a pivotal role in generating the dynamic correlation matrix  $\mathbf{C}_t$ . In practice, the selection of base kernels should be data-specific, and one should perform residual analysis to determine the most appropriate structure. For simplicity, we use  $M = 4$  base kernels—three SE kernels with  $l = 1, 2, 3$ , respectively, and an identity matrix. The different lengthscales capture different decaying rates of autocorrelation. The time-varying component weights can help the model dynamically adjust to different correlation structures observed at different time points. We use the Continuous Ranked Probability Score (CRPS) (Gneiting and Raftery, 2007) as the evaluation metric for uncertainty quantification:

$$\text{CRPS}(F, y) = \mathbb{E}_F |Y - y| - \frac{1}{2} \mathbb{E}_F |Y - Y'|, \quad (13)$$

where  $y$  is the observation,  $F$  is the cumulative distribution function (CDF) of a random variable  $Y$ , which is the target time series variable  $z_t$  in our case. For a clearer demonstration, we use  $\text{CRPS}_{\text{sum}}$  calculated by first summing CRPS across the entire testing horizon of all time series and then normalizing the result by the sum of the corresponding observations. Detailed information on the calculation of the CRPS is available in the supplementary materials.

In Table 1, we present a comparative analysis of prediction performance using DeepAR and Transformer as base models. The variants combined with our proposed method are compared to their respective original implementations optimized with Gaussian likelihood loss. The results demonstrate the effectiveness of our approach in enhancing the performance of both models across a wide range of datasets, yielding notable improvements in predictive accuracy. Our method yields an average improvement of 8.80% for DeepAR and 9.76% for Transformer. It should be noted that our method exhibits versatile performance improvements that vary across different datasets. This variability can be attributed to a combination of factors, including the inherent characteristics of the data and the baseline performance of the original model on each specific dataset. Notably, when the original model already achieves exceptional performance on a particular dataset, our method could demonstrate minimal enhancement (e.g., `uber_daily` and `uber_hourly`). Additionally, the alignment between the actual error autocorrelation structure and our kernel assumption also plays a pivotal role in influencing the performance of our method. Further analyses with other evaluation metrics (e.g. MSE and quantile loss) are reported in supplementary material.

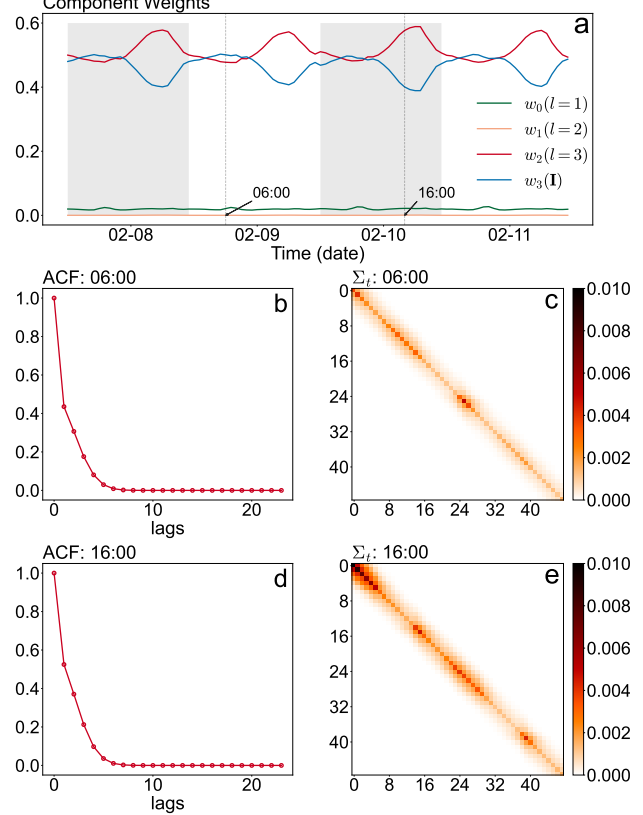


Figure 3: (a) Component weights for generating the correlation matrix of an example time series from the `m4_hourly` dataset. Parameters  $w_0, w_1, w_2$  represent the component weights for kernel matrices associated with lengthscales  $l = 1, 2, 3$ , respectively, and  $w_3$  is the component weight for the identity matrix. Shaded areas distinguish different days; (b) and (d): The auto-correlation function (ACF) indicated by the resulting error correlation matrix  $\mathbf{C}_t$  at 6:00 and 16:00. Given the rapid decay of the ACF, we only plot 24 lags to enhance clarity in our visualization; (c) and (e): The corresponding covariance matrix of the associated target variables  $\Sigma_t = \text{diag}(\boldsymbol{\sigma}_t) \mathbf{C}_t \text{diag}(\boldsymbol{\sigma}_t)$  at 6:00 and 16:00, respectively.

### 5.3 Interpretation of Correlation

A key element of our method lies in its ability to capture error autocorrelation through the dynamic construction of a covariance matrix. This is achieved by introducing a dynamic weighted sum of kernel matrices with different lengthscales. The choice of lengthscale significantly influences the structure of autocorrelation—a small lengthscale corresponds to short-range positive autocorrelation, while a large lengthscale can capture positive correlation spanning long lags.

In Fig. 3, we present the generated component weights

Table 1: CRPS<sub>sum</sub> accuracy comparison (lower is better, better performance is in boldface). “w/o” implies the original implementation of models optimized with Gaussian likelihood loss, whereas “w/” implies the model combined with our method. Mean and standard deviation were obtained by running each model three times.

	DeepAR			Transformer		
	w/o	w/	rel. impr.	w/o	w/	rel. impr.
<code>m4.hourly</code>	0.1529 $\pm$ 0.0011	<b>0.1421<math>\pm</math>0.0003</b>	7.06%	0.1487 $\pm$ 0.0011	<b>0.1431<math>\pm</math>0.0009</b>	3.77%
<code>exchange_rate</code>	0.0069 $\pm$ 0.0001	<b>0.0059<math>\pm</math>0.0000</b>	14.49%	0.0081 $\pm$ 0.0001	<b>0.0074<math>\pm</math>0.0001</b>	8.64%
<code>m1.quarterly</code>	0.3767 $\pm$ 0.0006	<b>0.3076<math>\pm</math>0.0018</b>	18.34%	0.4449 $\pm$ 0.0034	<b>0.3302<math>\pm</math>0.0046</b>	25.78%
<code>pems03</code>	0.0870 $\pm$ 0.0000	<b>0.0811<math>\pm</math>0.0000</b>	6.78%	0.0907 $\pm$ 0.0000	<b>0.0845<math>\pm</math>0.0001</b>	6.84%
<code>pems08</code>	0.0650 $\pm$ 0.0001	<b>0.0588<math>\pm</math>0.0000</b>	9.54%	0.0622 $\pm$ 0.0000	<b>0.0591<math>\pm</math>0.0001</b>	4.98%
<code>solar</code>	0.7627 $\pm$ 0.0008	<b>0.7063<math>\pm</math>0.0005</b>	7.39%	0.6657 $\pm$ 0.0010	<b>0.5379<math>\pm</math>0.0010</b>	19.20%
<code>traffic</code>	0.2765 $\pm$ 0.0001	<b>0.2387<math>\pm</math>0.0001</b>	13.67%	0.2422 $\pm$ 0.0002	<b>0.2036<math>\pm</math>0.0001</b>	15.94%
<code>uber_daily</code>	0.0897 $\pm$ 0.0003	<b>0.0890<math>\pm</math>0.0001</b>	0.78%	0.0827 $\pm$ 0.0003	<b>0.0827<math>\pm</math>0.0002</b>	0.00%
<code>uber_hourly</code>	0.1549 $\pm$ 0.0007	<b>0.1532<math>\pm</math>0.0005</b>	1.10%	0.1503 $\pm$ 0.0007	<b>0.1462<math>\pm</math>0.0008</b>	2.73%
	avg. rel. impr.			avg. rel. impr.		
			8.80%			9.76%

and the resulting autocorrelation function (i.e., the first row in the learned correlation matrix  $\mathbf{C}_t$ ) as an example time series from the `m4.hourly` dataset over a four-day duration. In particular, we observe that the component weights  $(w_0, w_1)$  corresponding to the kernel matrices with  $l = 1$  and  $l = 2$  consistently hover near zero throughout the entire observation period. This suggests that the prevailing autocorrelation structure in this dataset is most effectively characterized by the kernel matrix associated with  $l = 3$ .

Furthermore, we observe the dynamic adjustment of correlation strengths facilitated by the identity matrix over time. Specifically, when  $w_3$  (weight assigned to the identity matrix) increases, the error process tends to exhibit greater independence. In contrast, when the weight  $w_2$  for the kernel matrix with  $l = 3$  is larger, the error process becomes more correlated. Figs. 3 (b, d) reveal that the autocorrelation at 6:00 in the morning is less pronounced compared to that observed at 16:00. Additionally, Fig. 3 (a) demonstrates pronounced daily patterns in autocorrelation, particularly when errors exhibit an increased correlation around 18:00 each day. This underscores the crucial need for our methodology to dynamically adapt the covariance matrix, enabling the effective modeling of these temporal variations. Figs. 3 (c, e) illustrate the corresponding covariance matrix of the associated target variables within the autocorrelation horizon. The diagonal elements represent the variance of the target variables generated by the base model, while the off-diagonal elements depict the covariance of the target variables that are facilitated by our approach.

## 6 CONCLUSION

This paper introduces a novel method to tackle error autocorrelation in probabilistic time series fore-

casting. The method involves using mini-batches in training and learning a time-varying covariance matrix that captures the correlation among normalized errors within a mini-batch. Taken together with the standard deviation provided by the base model, we are able to model and predict a time-varying covariance matrix. We implement and evaluate the proposed method using DeepAR and Transformer on various public datasets, and our results confirm the effectiveness of the proposed solution in improving the quality of uncertainty quantification. The broader impact of our method can be observed in two aspects. First, since Gaussian errors are commonly assumed in probabilistic forecasting models, our method can be applied to enhance the training process of such models. Second, the learned autocorrelation can be leveraged to improve multi-step prediction by calibrating the distribution output at each forecasting step.

There are several directions for future research. First, the kernel-based covariance matrix may be too restrictive for capturing temporal processes. Exploring more flexible covariance structures, such as parameterizing  $\mathbf{C}_t$  as a fully learnable positive definite symmetric Toeplitz matrix (e.g., AR( $p$ ) process has covariance with a Toeplitz structure) and directly factorizing the covariance matrix  $\mathbf{\Sigma}_t = \mathbf{U}_t \mathbf{U}_t^\top$  (e.g., Wishart process as in Wilson and Ghahramani (2011)) or the precision matrix  $\mathbf{\Lambda}_t = \mathbf{\Sigma}_t^{-1} = \mathbf{V}_t \mathbf{V}_t^\top$  (e.g., using Cholesky factorization as in Fortuin et al. (2020)), could be promising avenues. Second, our method can be extended to multivariate models, in which the target output becomes a vector instead of a scalar. A possible solution is to use a matrix Gaussian distribution to replace the multivariate Gaussian distribution used in the current method. This would allow us to learn a full covariance matrix between different target series, thereby capturing any cross-correlations between them.

## References

Alexandrov, A., Benidis, K., Bohlke-Schneider, M., Flunkert, V., Gasthaus, J., Januschowski, T., Maddix, D. C., Rangapuram, S., Salinas, D., Schulz, J., et al. (2020). Gluonts: Probabilistic and neural time series modeling in python. *The Journal of Machine Learning Research*, 21(1):4629–4634.

Beitner, J. (2020). Pytorch forecasting. <https://pytorch-forecasting.readthedocs.io>.

Benidis, K., Rangapuram, S. S., Flunkert, V., Wang, Y., Maddix, D., Turkmen, C., Gasthaus, J., Bohlke-Schneider, M., Salinas, D., Stella, L., et al. (2022). Deep learning for time series forecasting: Tutorial and literature survey. *ACM Computing Surveys*, 55(6):1–36.

Choi, S., Saunier, N., Trepanier, M., and Sun, L. (2022). Spatiotemporal residual regularization with dynamic mixtures for traffic forecasting. *arXiv preprint arXiv:2212.06653*.

de Bézenac, E., Rangapuram, S. S., Benidis, K., Bohlke-Schneider, M., Kurle, R., Stella, L., Hasson, H., Gallinari, P., and Januschowski, T. (2020). Normalizing kalman filters for multivariate time series analysis. *Advances in Neural Information Processing Systems*, 33:2995–3007.

Fortuin, V., Baranchuk, D., Rätsch, G., and Mandt, S. (2020). Gp-vae: Deep probabilistic time series imputation. In *International conference on artificial intelligence and statistics*, pages 1651–1661. PMLR.

Gneiting, T. and Raftery, A. E. (2007). Strictly proper scoring rules, prediction, and estimation. *Journal of the American statistical Association*, 102(477):359–378.

Hamilton, J. D. (2020). *Time Series Analysis*. Princeton University Press.

Huang, Q., He, H., Singh, A., Lim, S.-N., and Benson, A. R. (2020). Combining label propagation and simple models out-performs graph neural networks. *arXiv preprint arXiv:2010.13993*.

Hyndman, R. J. and Athanasopoulos, G. (2018). *Forecasting: Principles and Practice*. OTexts.

Jia, J. and Benson, A. R. (2020). Residual correlation in graph neural network regression. In *Proceedings of the 26th ACM SIGKDD International Conference on Knowledge Discovery & Data Mining*, pages 588–598.

Prado, R., Ferreira, M. A., and West, M. (2021). *Time Series: Modeling, Computation, and Inference*. CRC Press.

Radford, A., Narasimhan, K., Salimans, T., Sutskever, I., et al. (2018). Improving language understanding by generative pre-training.

Rangapuram, S. S., Seeger, M. W., Gasthaus, J., Stella, L., Wang, Y., and Januschowski, T. (2018). Deep state space models for time series forecasting. *Advances in neural information processing systems*, 31.

Rasul, K., Seward, C., Schuster, I., and Vollgraf, R. (2021). Autoregressive denoising diffusion models for multivariate probabilistic time series forecasting. In *International Conference on Machine Learning*, pages 8857–8868. PMLR.

Rasul, K., Sheikh, A.-S., Schuster, I., Bergmann, U., and Vollgraf, R. (2020). Multivariate probabilistic time series forecasting via conditioned normalizing flows. *arXiv preprint arXiv:2002.06103*.

Saha, A., Basu, S., and Datta, A. (2023). Random forests for spatially dependent data. *Journal of the American Statistical Association*, 118(541):665–683.

Salinas, D., Bohlke-Schneider, M., Callot, L., Medico, R., and Gasthaus, J. (2019). High-dimensional multivariate forecasting with low-rank gaussian copula processes. *Advances in neural information processing systems*, 32.

Salinas, D., Flunkert, V., Gasthaus, J., and Januschowski, T. (2020). Deepar: Probabilistic forecasting with autoregressive recurrent networks. *International Journal of Forecasting*, 36(3):1181–1191.

Sun, F.-K., Lang, C., and Boning, D. (2021). Adjusting for autocorrelated errors in neural networks for time series. *Advances in Neural Information Processing Systems*, 34:29806–29819.

Tang, B. and Matteson, D. S. (2021). Probabilistic transformer for time series analysis. *Advances in Neural Information Processing Systems*, 34:23592–23608.

Wang, Y., Smola, A., Maddix, D., Gasthaus, J., Foster, D., and Januschowski, T. (2019). Deep factors for forecasting. In *International conference on machine learning*, pages 6607–6617. PMLR.

Wen, R., Torkkola, K., Narayanaswamy, B., and Madeka, D. (2017). A multi-horizon quantile recurrent forecaster. *arXiv preprint arXiv:1711.11053*.

Wilson, A. G. and Ghahramani, Z. (2011). Generalised wishart processes. In *Proceedings of the Twenty-Seventh Conference on Uncertainty in Artificial Intelligence*, pages 736–744.

Zhan, W. and Datta, A. (2023). Neural networks for geospatial data. *arXiv preprint arXiv:2304.09157*.

Zheng, V. Z., Choi, S., and Sun, L. (2023). Enhancing deep traffic forecasting models with dynamic regression. *arXiv preprint arXiv:2301.06650*.